Learning-based approach for the automatic detection of the optic disc in digital retinal fundus photographs

Damon Wing Kee WONG, Jiang LIU, Ngan Meng TAN, Fengshou YIN, Beng-Hai LEE, Tien Yin WONG

***Abstract*—The optic disc is an important feature in the retina. We propose a method for the detection of the optic disc based on a supervised learning scheme. The method employs pixel and local neighbourhood features extracted from the ROI of a digital retinal fundus photograph. A support vector machine based classification mechanism is used to classify each image point as belonging to the cup and retina. The proposed method is evaluated on a sample image set of 68 retinal fundus images. The results show a high correlation (r>0.9) with the ground truth segmentation, with an overlap error of 6.02%, and found to be comparable to the inter-observer variability based on an independent second observer segmentation of the same data set.**

I. Introduction

THE optic nerve head, is a key anatomical feature in the retina[1]. In the retina is a layer of cones and rods which are the photoreceptors responsible for sight. The retinal ganglion cells are the nerve cells which transmit visual information from the photoreceptors to the brain. As the ganglion cells exit the retina, they bundle together to form the optic nerve. The exit point at the retina is known as the optic nerve head, or optic disc. In a typical retinal fundus image, the optic disc can be viewed as an elliptical region of lighter intensity than the surrounding retina.

The detection and localization of the optic disc has many applications. As a key feature in retinal fundus images, the optic disc is often used as the principal landmark from which subsequent processes are dependent upon. For example, in [2], the location of the optic disc relative to the macula is useful to determine if an image is from the left or right eye. Also, the optic disc can be viewed as the entrance point of major vessels, or arcades, into the retina, which can be useful for retinal vessel tracking. Fig 1 shows a typical retinal fundus image with the major features indicated.

In addition to physiological information, accurate detection of the optic disc is also useful in many computer aided diagnosis applications. For example, in glaucoma, degenerative changes can be found within the optic disc, specifically changes in the size of the optic cup, and without the disc, such as beta peripapillary atrophy and retinal nerve fiber layer changes. In pathological myopia, the tilt of the optic disc is an important characteristic to determine the severity of myopia. And in diabetic retinopathy, the size and location of the disc is useful in quantifying vascular changes. The detection of the optic disc remains a main step in the development of automated systems for screening. One approach for disc detection has been to utilize vascular information since the optic disc can be seen as a point of convergence of the vascular architecture in the retina [3-5]. Hoover et al[3] employed a fuzzy geometry technique to determine convergence, while Youssif et al[4] used vessel direction as a vector for disc detection. Foracchia[5] et al implemented a model based on vessel structure to determine the location of the optic disc.

Besides vascular convergence, the optic disc can be detected by using the inherent properties of the optic disc such as its brightness and shape. In [6], disc detection was performed on scanning laser tomography images by combining these properties with an active contour model. Muramatsu et al [7] employed a similar approach using color channel information fitted with Snakes active contour method in stereoscopic retinal fundus images. Also using stereo images, Abramoff et al [8] automatically segmented the optic disc through the use of pixel features via a kNN classifier. Using only non-stereoscopic images, Inoue et al [9] performed disc detection via intensity thresholding, while Zhu and Rangayyan [10] made use of a Hough transform technique to delineate the optic disc, again based on intensity. In our previous work[11], we have developed a method for optic disc detection through a variational level set technique which employs information in the red channel, with the contours refined through ellipse fitting.

In this paper, we report a method for automatic detection of the optic disc through a supervised learning approach. The method utilized employs pixel-based classification through pixel and pixel neighbourhood features. To test the performance of the method, we assess it on a retinal image

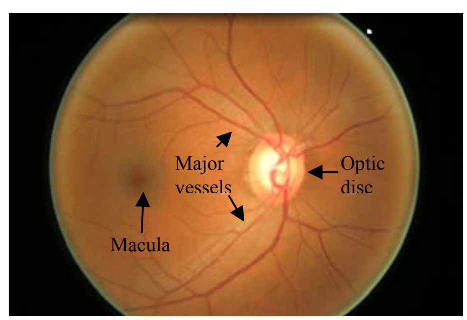

D.W.K. Wong, J.Liu, N.M. Tan, F. Yin and B.H. Lee are with the Institute for Infocomm Research, A*STAR, Singapore (phone: (065)6408-2526; fax: (065)6776-1378; e-mail:wkwong@ i2r.a-star.edu.sg).

T.Y. Wong is with the Singapore Eye Research Institute and the National University of Singapore.

Fig. 1. Typical anatomical features in a digital retinal fundus photograph

data set in which the optic disc has been segmented by a team of experienced graders. Inter-observer variability on the data set is also evaluated with a second observer.

II. Proposed Method

In this section, we describe the proposed automated optic disc detection method. First, a region of interest (ROI) is extracted from the retinal fundus image. Subsequently, this ROI is processed to extract pixel and neighbourhood features from which optic disc detection is performed in a supervised learning method using support vector machines.

A. ROI Detection

Typically, an optic disc occupies less than 10% of the retinal image. As the proposed method is focused on optic disc detection, it would be computationally inefficient to process the entire retinal fundus image to detect the optic disc. Instead, we first detect a region of interest centred on the optic disc by considering the histogram of the retinal fundus image. As the optic disc tends to be of higher intensity than the rest of retina image, we select the brightest 5% of the pixels, and the centroid of these selected pixels as the centre of the 800x800 pixel ROI. The ROI is then downsampled to 100x100.

B. Feature Extraction

For each image point i in the ROI, $i:[1,m]$, $i \subseteq \mathbb{Z}^+$ and where m is the total number of pixels in the ROI, a number of features are extracted to be used in subsequent classification, selected based on the visual appearance of the optic disc and surrounding retina. The color information is highly discriminative, due to the different colorFor pixel-based features, we employed the red *R(i)*, green *G(i)*and blue *B(i)* color channel information from the ROI. In addition, grayscale information *Y(i)* was also found to be useful due to the observed increased brightness of the optic disc compared to the surrounding retina. *Y(i)* was obtained from the RGB channel using $Gy(i)=\alpha R(i)+\beta G(i)+\gamma B(i)$. Typical values were used for the conversion i.e. $\alpha=0.30$, $\beta=0.59$, $\gamma=0.11$.

Besides intensity features, two additional features were used calculated to quantify the observable difference in 'roughness' between the optic disc and surrounding retina. Entropy is a measure of statistical randomness that can be used to characterize the degree of randomness or ‘roughness’ in an image. Considering S as the set 3x3 pixels in the neighbourhood of each pixel i, the entropy E is calculated as $E(i) = \Sigma(p*\log_2(p))$. The standard deviation of

TABLE I
FEATURES USED FOR CLASSIFICATION

Symbol	Quantity
R	Red channel
G	Green channel
B	Blue channel
Y	Gray channel
E	Local entropy
S	Local contrast

the set S for each pixel i was also calculated as a measure of the local

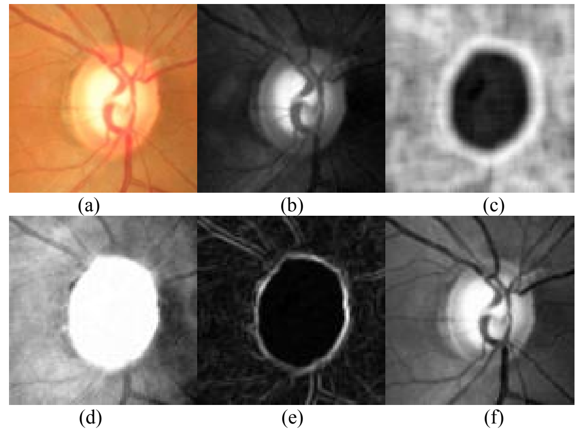

Fig. 2. Feature space representations of the ROI. (a) Original color, (b) red color channel (c) green color channel, (d) blue color channel, (e)local entropy and (f) local contrast. The images in this figure have been scaled to present maximum contrast.

contrast, and is denoted as D(i). The above features are summarized in Table I. Fig. 2 shows the maps for each of the features in Table I on a ROI obtained from a typical retinal fundus image.

C. Classification

Each of the pixels in the extracted ROI of a retinal fundus image can be considered as potentially belonging to the optic disc, and the decision can be considered as a classification problem. To classify each pixel as a disc or non-disc pixel, we adopted a supervised machine learning scheme based on support vector machines.

Support vector machines (SVM) techniques are widely used in many fields, including bioinformatics and computer vision applications. In SVM, the objective is to determine the optimal hyperplane, which can separate inputs into two or more classes. This optimal hyperplane is formed by identifying the supporting vectors which maximize a parallel margin between two or more classes. Unlike neural networks, which can be a potentially unconstrained minimization problem, SVM-based classification can be treated as a quadratic programming problem with linear constraints, represented as

$$\min_{w,b,\xi} \quad \frac{1}{2}w^T w + C\sum_{i=1}^{N}\xi_i$$

$$\textit{subject to} \quad y_i\left(w^T\phi(x_i)+b\right) \geq 1-\xi_i$$
$$\xi_i \geq 0, i=1,...N$$

where x_i represent the training vectors, y_i is the class, N is the number of training samples, w and b are variables, and ξ is the slack variable to implement a soft margin, and C>0 is the penalty term. $\phi(.)$ is known as the kernel function which can aid in better separating the classes by transforming the data into a higher dimensional space.

In this paper, SVM was implemented via the LIBSVM[12] toolbox. Each pixel was used as an input into

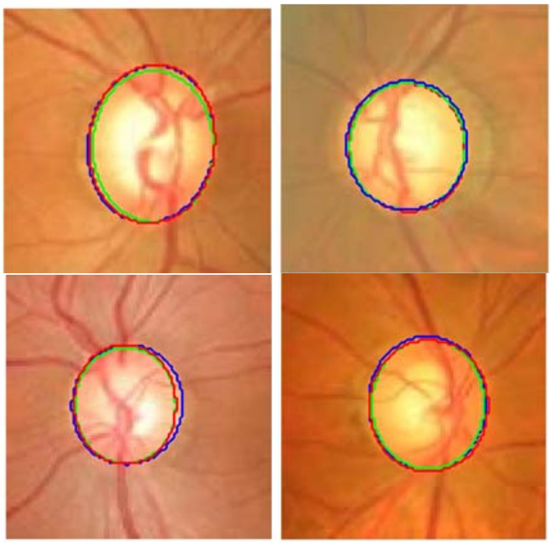

Fig. 3. Segmentation of the optic disc using the proposed automatic method (red), ground truth segmentation (green) and second observer (blue)

the SVM classifier, with a six-dimension feature vector based on the features in Table I. A radial basis function was selected for use to enhance separation of the inputs as belonging to the optic disc or the retina.

III. Experiments and Results

To train and test the system, we made use of a batch of 68 retinal fundus images from the Singapore Eye Research Institute. The images were during the Singapore Malay Eye Study (SiMES), a population-based survey of eye diseases in the Malay population over 40 in Singapore. Each retinal image has a resolution of 3072x2048 pixels, taken under clinical conditions. For each image, a team of experienced graders manually outlined the disc boundary. This segmentation set is defined as the ground truth segmentation which will be used to train and test the proposed method. In addition, a second segmentation was performed independently by an ophthalmologist, and is defined as the second observer segmentation. Both segmentations only relied on the retinal fundus image, with no additional clinical information or other modalities taken into account.

The image set was processed via the steps described in Section 2 for ROI detection and feature extraction for each image. Before the SVM classifier can be used, the model must first be trained. This involves selecting parameters which affect the accuracy and generalization performance of the model, and subsequently training the model using these parameters. In the SVM implementation, the values of the cost function C and γ, which is related to the radial basis function, are chosen through a grid search procedure. In this method, a range of possible values of C and γ are fixed, and the model performance is evaluated. For the grid search, a set of 30,000 labeled representative image points was used to evaluate each C and γ value, with 5-fold cross validation performed at each search point. The selected C and γ

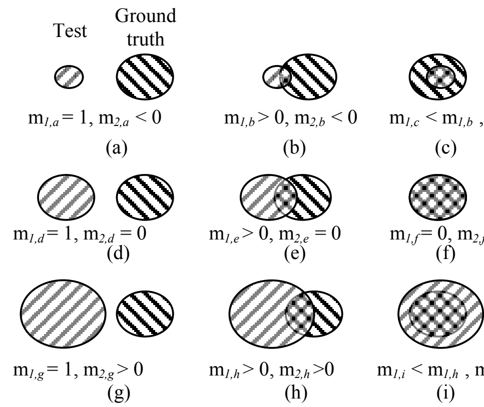

Fig. 4. Illustration of the implications for varying values of m_1 and m_2, taking with respect to the shown ground truth examples.

produced a cross validation accuracy of 99% in the data set. These parameters were used during the training phase, in which the SVM model was trained on a set of ten images. Subsequently, the full image set of 68 images was input into the trained SVM model, and the optic disc was determined for each image. Morphological open and close operations were performed, followed by fitting the detected optic disc boundary to an ellipse to reduce boundary irregularities. Examples of the automated optic disc segmentations together with the ground truth and second observer disc segmentations are shown in Fig. 3. The segmentation results show a good detection of the optic disc even for differing color tones of the fundus image.

To quantify the performance of the optic disc segmentation by the proposed method, a number of performance metrics were used. The area overlap error, m_1, is defined as

$$m_1 = \left(1 - \frac{Area_{seg} \cap Area_{ref}}{Area_{seg} \cup Area_{ref}}\right) \times 100\% \qquad (1)$$

where $Area_{seg}$ indicates the segmented area by our system, and $Area_{ref}$ denotes the reference area, or ground truth segmentation. The area overlap error metric is an indicator of how well the segmented area matches with the reference area, where a m_1 value of '0' indicates perfect segmentation in which the segmented area overlaps perfectly with the reference segmentation, and a value of '1' indicates totally no overlap. Although m_1 is a useful gauge of segmentation performance, it is non-negative, and will be unable to indicate over or under segmentation. This is particularly the case when either the segmented area completely overlaps the reference area, or vice versa. A useful metric to complement m1 is the relative area difference m_2, defined as

$$m_2 = \frac{Area_{seg} - Area_{ref}}{Area_{ref}} \times 100\% \quad (2)$$

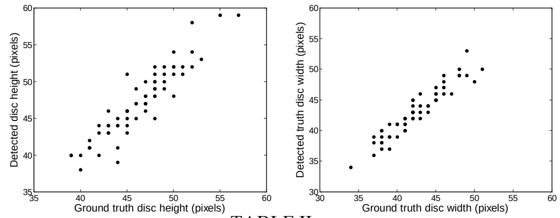

Fig. 5. Comparison of the vertical (left) and horizontal (right) optic disc dimensions using the automated disc detection method (y-axis) and ground truth optic disc (x-axis).

TABLE II
PERFORMANCE METRICS (WRT GROUND TRUTH)

Metric	Proposed automatic disc detection	2nd observer
m_1	6.0251%	8.7036%
m_2	<0	>0
$\lvert m_2 \rvert$	4.2704%	8.4427%
Optic disc height correlation	0.931	0.948
Optic disc width correlation	0.939	0.945
RMSE for disc height	2.04 pixels	2.41 pixels
RMSE for disc width	1.36 pixels	2.34 pixels

The relative area difference indicates if a segmentation is under- or over- segmented by its sign (m_2>0: under-segmentation; m_2<0: over-segmentation) as well the extent of area difference by its magnitude. Conveniently, similar to m_2, a value of 0 indicates no error in the size of the segmented area. Illustrations of various possibilities and the accompanying values of m_1 and m_2 are shown in Fig. 4.

The size of the automatically detected optic disc segmentations was also compared to the ground truth segmentation and the results are plotted in Fig. 5. To assess the accuracy of the detected dimensions, we calculated the root mean square error (RMSE) of the detected optic disc dimensions with respect to the ground truth segmentation. In the analysis, we also calculated the correlation for the disc dimensions between the automatic segmentation and the ground truth segmentation using Spearman's correlation coefficient, where a higher value of indicates and stronger correlation, and vice versa. The average performance metrics of the results on the data set are tabulated in Table II. The average of the absolute values of m_2 is also provided to give an indication of the overall error in the segmentation. To assess the inter-observer variability on the optic disc identification on the image data-set, the previously described metrics were also calculated for the 2nd observer segmentation taken with respect to the ground truth.

From the values presented in Figure 1, it can be observed that the proposed method achieves an overlap error (m_1) of about 6%, which is within the inter-observer error of 8.7%. Furthermore, the automatically detected optic disc tends to over-segment the optic disc (m_2>0) with an average size error of about 4.3%. In comparison, the inter-observer assessment shows on average an overestimation on the disk size of about 8.4%.The results also show a high correlation for both disc height and disc width for the automatic disc detection (r>0.9), with a RMSE error of 2.04 and 1.36 pixels for the disc height and width respectively. The results of the proposed system are comparable to the inter-observer correlation and RMSE for both dimensions.

IV. CONCLUSION

The optic disc is an important anatomical feature in the retina, and acts as a key contextual landmark for other anatomical features, as well as disease pathologies such as glaucoma. In this work, we have presented a method for automated detection of the optic disc in retinal fundus images through the use of a supervised learning scheme. The method utilizes pixel and local features to classify image points using a support vector machine based classification mechanism. Experimental results show that the method is able to achieve a high accuracy and correlation with the ground truth segmentation, and is comparable to inter-observer variability based on segmentation from a second observer. The results are promising for the further development of the method for automated detection of the optic disc in retinal fundus images.

REFERENCES

[1] R.R. Allingham, K.F. Damji, S. Freedman, S.E. Moroi, G. Shafranov, *Shields' Textbook of Glaucoma*, 5th Edition. Lippincott Williams & Wilkins, 2005.

[2] N.M. Tan, J. Liu, D.W.K. Wong, Z. Zhang, S. Lu, J.H. Lim and H. Li, "Classification of left and right eye retinal images," *Proc. SPIE*, Vol. 7624, 762438, 2010.

[3] A. Hoover, M. Goldbaum, "Locating the optic nerve in a retinal image using the fuzzy convergence of the blood vessels," IEEE Trans Med Imaging. 2003 Aug;22(8):951-8.

[4] A.R. Youssif A.Z. Ghalwash, A.R. Ghoneim, "Optic disc detection from normalized digital fundus images by means of a vessels' direction matched filter," IEEE Trans Med Imaging. 2008 Jan;27(1):11-8.

[5] M. Foracchia, E. Grisan, A. Ruggeri, "Detection of optic disc in retinal images by means of a geometrical model of vessel structure," IEEE Trans Med Imaging. 2004 Oct;23(10):1189-95.

[6] R. Chrástek, M. Wolf, K. Donath, H. Niemann, D. Paulus, T. Hothorn, B. Lausen, R. Lämmer, C.Y. Mardin, G. Michelson G, "Automated segmentation of the optic nerve head for diagnosis of glaucoma," *Med Image Anal*. 2005 (4):297-314.

[7] C.Muramatsu, T.Nakagawa, A.Sawada, Y.Hatanaka, T.Hara, T.Yamamoto, and H.Fujita, "Determination of cup and disc ratio of optical nerve head for diagnosis of glaucoma on stereo retinal fundus image pairs," *Proc. of SPIE*, 7260, 72603, 2009.

[8] M.D. Abramoff, W.L.M. Alward, E.C. Greenlee, L. Shuba, C.Y. Kim, J.H. Fingert, Y.H. Kwon, "Automated Segmentation of the Optic Disc from Stereo Color Photographs Using Physiologically Plausible Features," *Inves. Oph. Vis. Sci.,* 2007, 48, 1665-1673.

[9] N. Inoue, K. Yanashima, K. Magatani, T. Kurihara, "Development of a simple diagnostic method for the glaucoma using ocular Fundus pictures," *Conf Proc IEEE Eng Med Biol Soc*. 2005;4:3355-8.

[10] X. Zhu, R.M. Ranggayyan, "Detection of the optic disc in images of the retina using the Hough transform," Conf Proc IEEE Eng Med Biol Soc. 2008;2008:3546-9.

[11] D.W.K. Wong, J. Liu, J.H. Lim, X. Jia, F. Yin, H. Li, T.Y. Wong, " Level-set based automatic cup-to-disc ratio determination using retinal fundus images in ARGALI," *Conf Proc IEEE Eng Med Biol Soc.* 2008;2008:2266-9

[12] C.-C. Chang and C.-J. Lin, LIBSVM : a library for support vector machines, 2001.